Redox-triggerable Luciferin-Bioinspired Hydrogels as Injectable and Cell-encapsulating Matrices

Minye Jin[1,2,3], Alisa Gläser[1], and Julieta I. Paez[1,3]*

[1] INM – Leibniz Institute for New Materials. Campus D2-2, 66123, Saarbrücken, Germany.

[2] Chemistry Department, Saarland University. 66123, Saarbrücken, Germany.

[3] Developmental Bioengineering, TechMed Centre and Molecules Centre, University of Twente. Drienerlolaan 5, 7522 NB, Enschede, The Netherlands.

Corresponding author (*): Dr. Julieta I. Paez, email: j.i.paez@utwente.nl

Graphical abstract:

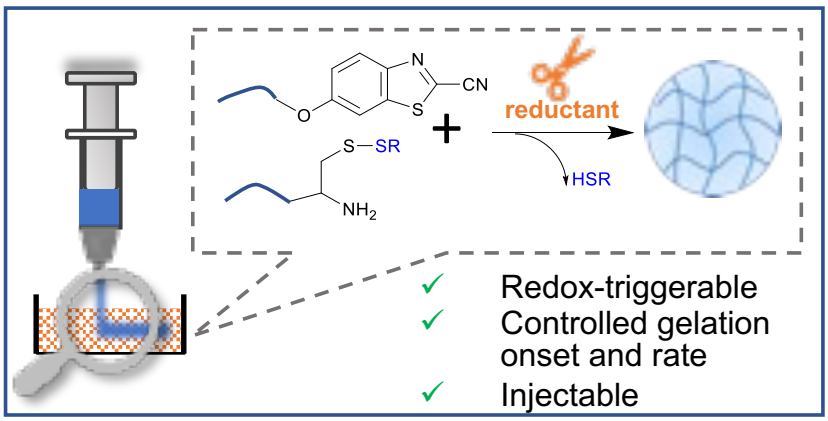

A novel redox-triggered bioinspired hydrogel is presented, which offers high control over gelation onset and kinetics. This platform is suitable for the development of injectable matrices.

Abstract

Over the past few decades there has been a great interest in developing smart hydrogels that are stimuli-responsive, due to their ability to respond to variations caused by external stimuli. These materials are exploited for biomedical applications such as biosensors, injectable scaffolds, drug delivery and tissue engineering. Recently, our group reported firefly-inspired hydrogel matrices for 3D cell culture. This platform exhibited certain advantages like rapid gelation rate and tunability of mechanical and biological properties. However, this firstly reported system did not allow for fine control of the gelation onset because the crosslinking reaction started as soon as the two precursors were mixed. Moreover, one of its precursors demonstrated poor storage stability in aqueous solution. These limitations restrict its application as injectable matrices. In this article, we endow the luciferin-inspired hydrogels with redox-triggering capability, to overcome the limitations of the previous system and to widen its application range. We achieve this goal by introducing protected macromers as hydrogel polymeric precursors that can be activated in the presence of a mild reductant, to trigger gel formation in situ with high degree of control. We demonstrate that the regulation of intrinsic (e.g., structure of protecting group, reductant type) and extrinsic (e.g., pH, temperature) parameters of the triggering reaction can be used to modulate key materials properties. This novel upgraded redox-triggerable system enables precise control over gelation onset and kinetics, thus facilitating its utilization as injectable hydrogel without negatively impacting its cytocompatibility. Our findings expand the current toolkit of chemically-based stimuli-responsive hydrogels.

Keywords: Hydrogels, Redox-responsive materials, Injectability, Gelation rate, Bioinspired materials

1. Introduction

Hydrogels are porous hydrophilic crosslinked networks. Due to their high water content as well as highly tunable biophysical and biochemical properties, hydrogels have been used as extracellular matrix mimics in cell and therapeutics delivery, as in vitro disease models, for tissue gluing and tissue engineering.[1-3] In particular, the introduction of stimuli-responsive features in the hydrogel design has attracted interest for the development of smart biomaterials for various medical applications. Thereby, stimuli-responsive hydrogels that experience changes in their equilibrium swelling,[4] undergo sol-gel[5] or gel-sol transition,[6] or can modify their bioactivity[7] in response to an applied stimulus (also called "trigger") have been reported. Diverse physical (temperature,[8, 9] light,[6, 10] electrical, magnetic and ultrasound fields[11-13]) and chemical (pH,[14, 15] enzymes[16] and small molecules[17, 18]) triggers have been used to tune materials properties on demand. These smart biomaterials have been successfully implemented in a wide range of applications including biosensors, actuators, cell and drug delivery and scaffolds for tissue engineering.[19, 20]

Among chemically-responsive hydrogels, those systems that can be triggered or actuated by biocompatible redox reactions are promising for biomedical applications because of the easy access and cost-efficiency of redox triggers. For instance, redox-responsive functional groups in the hydrogel can react with mild oxidants or reductants, leading to either the formation or the cleavage of bonds, thus inducing changes in biomaterials properties.[21] One representative redox reaction applied for preparation of biocompatible systems is the catechol to quinone oxidation that is used to trigger sol-gel transition.[6] Another example is the thiol/disulfide pair. The thiol to disulfide oxidation can be applied for sol-gel transition or increase of crosslinking density,[22, 23] while the disulfide to thiol reduction is typically used for gel-sol transition or decrease of the crosslinking density.[24, 25] These strategies have mostly been implemented to modulate

mechanical properties on demand[24] as well as to promote controlled drug release[26] from the hydrogel matrix. Despite this exciting progress, one aspect that remains relatively unexplored in this field is the use of redox reactions to precisely trigger the onset as well as to control the rate of gelation process, without detriment of materials cytocompatibility. When implemented in the context of cell encapsulation, these redox-triggerable matrices with flexible control over gelation onset and rate are envisioned as versatile hydrogel platforms with tunable properties, with application potential as injectable matrices and printable hydrogel inks.

Recently, our group reported soft biomaterials whereby crosslinking chemistry was inspired by the biochemistry of fireflies.[27] A luciferin-inspired polyethylene glycol (PEG) based hydrogel for 3D cell culture was presented. These hydrogels were crosslinked via the so-called luciferin click ligation, which involves a condensation reaction between cyanobenzothiazole (CBT) and cysteine (Cys) groups. The resulting materials, termed as CBT-Cys hydrogels, exhibited efficient gelation rate under physiological conditions, high homogeneity at the microscale, good cytocompatibility and tunable mechanical strength within physiologically relevant values. Upon stem cell encapsulation and by regulating hydrogel's bioactivity through incorporation of biochemical cues (i.e., cell-adhesive and cell-degradable ligands), modulation of cell-materials interaction was achieved. Remarkably, the gelation rate of the system could be regulated within the seconds range by adjusting pH within the close-to-physiological range (i.e., from 8.0 to 6.6) without impacting the final mechanical strength.[27]

Despite the mentioned advantages, the CBT-Cys system presented some limitations regarding user-control over system's properties. First, it did not allow for control of the gelation onset since the crosslinking reaction starts as soon as CBT and Cys precursors are mixed. This could complicate its application as in situ curing injectable matrices where too fast gelation rate could

lead to clogging of the syringe during injection. Second, even at the lowest pH value of 6.6, quick gel formation was observed (i.e., gelation time remained consistently < 1 min). This short gelation time proved ideal for homogeneous encapsulation of cells in the scaffold for the preparation of in vitro culture models in a culture plate.[27] However, this time is too short for other biomedical scenarios requiring slower gelation rate (e.g., within minutes range) such as those involving injection and in situ crosslinking of matrices for therapeutic delivery, tissue adhesion and engineering.[28, 29] Third, we and others[30] found that under physiological media (e.g., in buffer pH 7.4) Cys precursors undergo oxidation of Cys groups to form disulfide bridges, which inactivates the reactivity of Cys groups towards CBT moieties over time. Consequently, Cys precursors had to be freshly prepared before gel formulation via luciferin-inspired crosslinking. If this chemical instability in buffer were solved, stock solutions of Cys precursor could be prepared at one time point and used later, which is convenient for certain applications involving hydrogel fabrication in combination with processing technologies. We envisioned that the introduction of redox-triggers to the CBT-Cys gels will enable to overcome all the mentioned limitations of the existing system. It will confer higher stability to precursors and allow for precise control of gelation onset and kinetics, thus facilitating this system's application as injectable matrices with flexible and tailorable properties.

In this article, we investigated whether the incorporation of redox-responsive moieties onto the Cys precursor of luciferin-inspired hydrogels could impart the system with redox-triggerable onset (as schematically shown in **Figure 1a**). To this end, the PEG-Cys precursor that contained terminal 1,2-aminothiol motifs, was chemically modified with a disulfide protecting group at the thiol rest to give a PEG-Cys(SR) precursor, therefore impeding the crosslinking reaction with PEG-CBT in aqueous conditions. Upon the addition of a mild reductant (i.e., the redox trigger), the protecting group was cleaved and free PEG-Cys was generated in situ, which in

the presence of PEG-CBT promoted hydrogelation. Here we demonstrate that tuning the disulfide cleavage reaction at the molecular level enables us to tightly modulate important materials properties such as gelation onset and kinetics, as well as mechanical strength of derived materials. Materials tunability can be done by tailoring intrinsic and extrinsic parameters of the deprotection reaction. Specifically, we studied the influence of the molecular structure of the PEG-Cys(SR) precursor, the reductant type used, and environmental cues such as pH and temperature; on the course of the gelation process. Working conditions for flexible preparation of cell-encapsulating hydrogels were found, while high viability of embedded stem cells was preserved. Finally, a proof of concept demonstrating that these redox-triggerable hydrogels can be formulated as injectable matrices with potential for the development of in-bath crosslinkable inks, is presented. These novel redox-triggerable bioinspired hydrogels with high user-control complement and expand the current palette of chemically-based stimuli-responsive systems. These biomaterials are expected to pave the way for innovative applications in the biomedical field.

2. Results and Discussion

Design and synthesis of PEG-Cys(SR) macromers for redox-triggerable gelation

We envisioned that thiol-protected PEG-Cys precursors will be key for the design of redox-triggerable hydrogels via luciferin-inspired crosslinking. We considered 4-arm PEG-Cys(SR) macromers presenting different protecting groups at the thiol residue (R= Et, tBu) and diverse molar masses (10 and 20 kDa). Different protecting groups (in this case, alkyl disulfides) are expected to show diverse cleavage rate in the presence of a reductant, thus enabling control over gelation kinetics. Additionally, the choice of precursor's molar mass was done to enable

tuning of important properties of derived materials (such as crosslinking degree and gelation rate), while leading to hydrogels that are adequate for cell encapsulation applications.[27, 31]

Control of the disulfide cleavage reaction at the molecular level was expected to allow fine tuning of materials properties at the micro/macroscopic level. According to reported work, the rate of disulfide cleavage depends on the chemical structure of the alkyl disulfide and on the specific reductant type used.[32-34] Regarding the structure of the disulfide protecting group, factors such as the steric hindrance and redox potential of the parent disulfide as well as pKa of the thiol leaving group are deemed important. Concerning the reductant type, parameters such as the redox potential of the reductant as well as the specific reaction mechanism taking place and the chemical orthogonality between reductant and CBT moiety,[27] are all aspects that could play a role in deprotection kinetics. In general, faster deprotection is attributed to smaller steric size of alkyl disulfide,[35] to lower pKa of the thiol leaving group,[36] and to the use of a stronger reductant. In our study, Cys precursor derivatives with different protecting groups were conceived: PEG-Cys(SR), R= Et or tBu. With smaller steric hinderance and lower pKa of thiol leaving group (HSEt = 10.6 vs. HStBu = 11.2), we anticipated faster deprotection rate and thus faster gelation rate for the system derived from the PEG-Cys(SEt) precursor. As for the reductant trigger, we used dithiothreitol (DTT), tris-(2-carboxyethyl)-phosphine (TCEP) and glutathione (GSH), which are widely used in chemical biology.[37] Note that, additionally, GSH exists in vivo and is used by living cells to regulate numerous redox processes.[38] Besides the distinct reduction potential of these three reductant,[39-41] it is important to mention the specific mechanism of disulfide cleavage. TCEP, a phosphine-based reductant, cleaves disulfide bonds via an irreversible mechanism that forms thiols and phosphine oxide.[42] In contrast, GSH and DTT, presenting thiol groups, cleave disulfide bonds through a disulfide-thiol exchange mechanism.[38, 39] Moreover, while the -COOH side groups of TCEP are foreseen chemically

orthogonal to CBT-Cys reaction, the thiol groups present in GSH and DTT might chemically interfere with the luciferin coupling as they can transiently react with CBT groups to form thioimidate adducts.[43] This could eventually delay the gelation time.

The PEG-Cys(SR) macromers were successfully synthesized in two steps from a commercial precursor PEG-amine (see scheme in Fig. 1b). Cys amino acid variants, presenting Boc protecting group at the amine rest and disulfide protecting groups at the thiol rest, had their free -COOH group activated with HBTU/HOBT mixture and were subsequently coupled to PEG-amine. The intermediate Boc-containing macromers showed a high substitution degree (> 90%), as revealed by ^{1}H-NMR spectroscopy. In a second step, the Boc group was removed in TFA:TIS:water (9.5:2.5:2.5) deprotection cocktail. Under these acidic conditions, the Boc group is selectively cleaved while the disulfide bond that protects the thiol rest remains stable. Successful Boc cleavage was proven by ^{1}H-NMR, by observing the disappearance of the signal of the Boc group at 1.42 ppm. After purification by dialysis and lyophilization, PEG-Cys(SEt) and PEG-Cys(StBu) macromers were obtained in 90% and 87% yield, respectively. Furthermore, PEG-CBT macromers (10 and 20 kDa) were prepared according to our previously published protocol.[27] Detailed description of the synthesis, purification, and characterization of the PEG macromers can be found in the ESI.

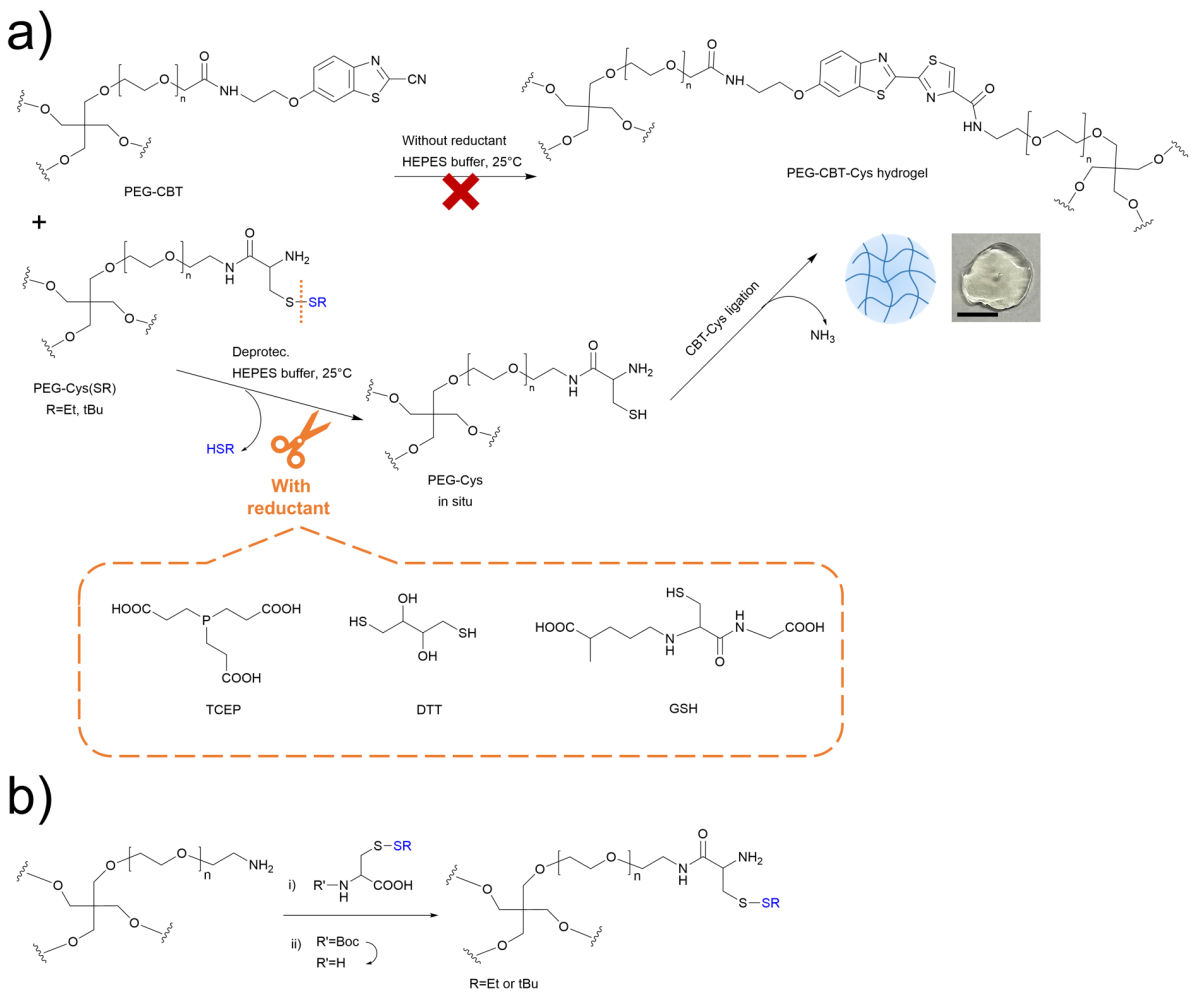

Figure 1. **a)** Schematics of the redox-triggered luciferin-bioinspired crosslinking, used in this work as a strategy for on-demand gelation. In the absence of a reductant, mixing PEG-CBT and PEG-Cys(SR) precursors does not lead to the formation of a hydrogel, because the thiol residue of Cys is protected. In contrast, the addition of a reductant cleaves the protecting group from PEG-Cys(SR) and generates PEG-Cys in situ, which in presence of PEG-CBT precursor leads to the formation of a hydrogel. The reductants used in this work, TCEP, DTT and GSH, are shown. A photography of a swollen PEG-Cys(SEt) gel at 3.3 wt% is included. Scale bar= 5 mm. **b)** Synthesis of PEG-Cys(SR) macromers. Reagents and conditions: i) HBTU, HOBT, DIPEA, dry DMF, room temp., 2 d; ii) TFA: triisopropylsilane (TIS): water (95: 2.5:2.5), room temp., 1.5 h.

PEG-Cys(SR) macromers show high stability in aqueous solution

Previously, we demonstrated that PEG-CBT macromers are stable in aqueous solution for at least 1 month.[27] Regarding the stability of PEG-Cys macromers, we noticed that solutions of these precursors had to be freshly prepared to avoid oxidation of thiols to disulfide bridges, which presumably leads to the inactivation of the macromer. Aged PEG-Cys solutions in buffer were unable to form CBT-Cys hydrogels upon mixing with PEG-CBT (see Fig. S1). The aqueous stability of precursors is relevant for the prospective storage of these compounds in solution, which could prove beneficial for the usage of these solutions in applications that require pre-mixing of precursors (e.g., injectable matrices and hydrogel inks in processing technologies). Therefore, we studied the stability of the PEG-Cys(SR) macromers in physiologically relevant medium: PEG-Cys(SR) precursor solutions were prepared in deuterated phosphate buffer saline (d-PBS) at pH 7.4 and at room temperature; and their ^{1}H NMR spectra were recorded over time up to 4 months. During this time, the solutions were stored under ambient conditions (i.e., room temperature and exposed to light from the laboratory). Both PEG-Cys(SEt) and PEG-Cys(StBu) compounds demonstrated high stability in aqueous conditions as no significant spectral change was observed within the investigated conditions (Fig. S1). Importantly, aged precursor solutions remained chemically reactive and formed hydrogels when mixed with PEG-CBT precursor. Altogether, these studies demonstrate the excellent stability of PEG-Cys(SR) precursors under physiologically relevant aqueous conditions that, in relation to PEG-Cys precursor, is advantageous for storage and pre-mixing of reactive macromer solutions.

Choice of protecting group and reductant type allows modulation of gelation onset and rate without affecting gel's final mechanical strength

Luciferin-inspired hydrogels were fabricated in 20 mM HEPES buffer at pH 8.0 under mild reductive conditions and using TCEP as reductant. First, 10 kDa PEG-CBT and PEG-Cys(StBu) precursor solutions at 3.3 wt% concentration were mixed at 1:1 volume ratio, and no hydrogel formation was observed (see Fig. S2), confirming that masking the thiol residue of the Cys group effectively prevents luciferin ligation. When 1 volume of TCEP reductant solution was added, to obtain a reactive mixture of final 5 wt% polymer concentration and CBT:Cys(SEt):TCEP (1:1:1) molar ratio; a hydrogel formed in 19 s, as revealed by a macroscopic test (**Table 1**). This proves that the addition of 1 equivalent of TCEP triggers the disulfide cleavage of PEG-Cys(SEt) precursor, thus unmasking the thiol moiety and triggering the formation of a hydrogel through luciferin click ligation. The formed hydrogels looked transparent and homogeneous to the naked eye and showed the pale-yellow color[27] that is characteristic of newly formed luciferin-like crosslinks (see picture of a hydrogel in insert of Fig. 1a).

Furthermore, when PEG-CBT was pre-mixed with PEG-Cys(StBu) followed by the addition of TCEP, a hydrogel formed in ~ 200 s (Table 1), which is about 10-fold slower than when PEG-Cys(SEt) was used as precursor. This indicates that, as expected, a bulkier protecting group at the thiol rest[35] as well as a higher pKa of the thiol leaving group[36] lead to slower disulfide cleavage, thus delaying the unmasking of the precursor and consequently decreasing the gelation rate. This finding validates the molecular design of the redox-triggerable Cys(SR) precursors. For comparison, a hydrogel obtained from mixing PEG-CBT and PEG-Cys (i.e., without protecting groups at the thiol rest of Cys) was prepared as control under the same conditions, observing a gelation time of 18 s. This indicates that the gelation rate obtained from

either of the two precursors, PEG-Cys(SEt) or PEG-Cys, is similar; which in turn evidences that the protecting group of PEG-Cys(SEt) can be cleaved very efficiently under these conditions.

Table 1. Gelation time points of different hydrogels at 5 wt% concentration, using TCEP as reductant, as measured by the macroscopic pipetting test.

Gel	CBT-Cys(SEt)	CBT-Cys(StBu)	CBT-Cys (control)
gelation time	18.6 ± 0.6 s	198.6 ± 7.7 s	17.3 ± 0.6 s

Conditions: 20 kDa, 5 wt% polymer concentration, in HEPES buffer at pH 8.0 containing 20 mM TCEP, T= 25 °C, n=3.

To further investigate the impact of the protecting group of the Cys(SR) variant on the gelation kinetics and mechanical strength of the hydrogels, the gelation of these materials was studied by oscillatory shear rheometry. In the following, the different hydrogels are denoted CBT-Cys(SR) when they are derived from PEG-Cys(SR) variants (R= Et, tBu) and named CBT-Cys when they are prepared from PEG-Cys precursor (control material).

A solution containing PEG-CBT and PEG-Cys(SR) was mixed directly on the bottom plate of the rheometer, followed by addition of TCEP solution and quick mixing, and the evolution of storage modulus (G') and loss modulus (G") was monitored over time at 25 °C (**Figure 2**). At 5 wt% concentration, formation of CBT-Cys(SEt) hydrogel was observed in the beginning of the experiment, indicated by G'>G". This evidences an efficient curing, with gelation time < 60 s (note that 60 s is the approx. time required for sample preparation and measurement setting), in good agreement with the values obtained by the macroscopic test shown on Table 1. In comparison, CBT-Cys(StBu) gels prepared under same conditions formed in ~3 min. During the curing process, G' increased and reached G'(Et)= 1334 Pa and G'(tBu)= 1191 Pa after 10 min (Fig. 2a). In a separate experiment, CBT-Cys(SR) gels of same composition were prepared

in molds, let cure for 120 min, then allowed to swell in buffer until equilibrium (~24 h), and the final mechanical strength of the gels after swelling was measured. CBT-Cys(SEt) and CBT-Cys(StBu) gels showed a shear modulus G' of 2202 and 2052 Pa, respectively; and the obtained G' values proved not significantly different indicating similar crosslinking density in both CBT-Cys(SEt) and CBT-Cys(StBu) gels (Fig. 2b). Overall, the observed trend in the gelation rate, CBT-Cys(Et) > CBT-Cys(StBu) reflects the rate of disulfide cleavage and deprotection of the Cys variants and demonstrates that the structure of the protecting group of the Cys precursor can be used to regulate the gelation time of derived materials from a few seconds to minutes. Importantly, this control of gelation onset and kinetics can be performed without altering the mechanics of CBT-Cys(SR) gels.

Next, we investigated the effect of the reductant type on the gelation process by rheometry. CBT-Cys(SEt) hydrogels were prepared at 3.3 wt% concentration, using TCEP, DTT or GSH as reductants, while keeping CBT:Cys(SEt):reductant (1:1:1) molar ratio. In this case, gelation time points measured by rheology were < 60 s, 5 min and 15 min, for TCEP, GSH and DTT, respectively. Moreover, G' evolved 90% in 5 min, 10 min and 60 min for gels containing TCEP, GSH, or DTT, respectively (Fig. 2c). Moreover, final G' values measured after swelling were 792, 977 and 842 Pa for TCEP, GSH and DTT systems, respectively, and these values were found not significantly different (Fig. 2d). This indicates that gelation rate followed the trend TCEP > GSH > DTT, while no significant difference in gel's mechanical strength was found after the swelling process. Interestingly, the gelation rate evidenced upon triggering by different reductants did not follow the trend of their reduction potential DTT (-0.33 V)[44], TCEP (-0.29 V)[40], and GSH (-0.26 V).[41] According to these values, it was expected that DTT would be the stronger reductant, leading to the most efficient disulfide cleavage and to the fastest redox-triggering; whereas our rheological characterization results suggest that DTT is the least

efficient of the reductants. This could indicate that in DTT other molecular effects such as competing side reactions, might play a role in the redox-triggering process. Worth nothing, our results are in agreement with kinetic data of reduction of aryl-disulfides in Tris buffer (100 mM, pH 8.2, at 25 °C), where reported cleavage rate followed the trend: TCEP > DTT > GSH.[33] This supports the idea that kinetics of disulfide cleavage does not solely depend on reduction potential of reductant. In line with previous work,[27] we hypothesize that redox-triggering by DTT is slower than expected because this reductant is not chemically orthogonal to the system since its thiol groups can engage in CBT-thiol reversible coupling.[12] DTT, a dithiol, is presumed to act both as a reductant and as a transient crosslinker, thus leading to redox-triggered CBT-Cys crosslinked networks with slower gelation rate. Altogether, our findings prove that the choice of reductant type also enables fine adjustment of the gelation rate without affecting final gel mechanics.

Furthermore, CBT-Cys(StBu) hydrogels prepared under same conditions evidenced gelation times generally slower than CBT-Cys(SEt) analogues and their gelation times also depended on the reductant used. At 3.3 wt% polymer concentration, gelation times for CBT-Cys(StBu) system of 27 min and 24 h were observed for TCEP and DTT, respectively; while no gel formation was obtained in the presence of GSH (Table S1). A faster gelation rate TCEP > DTT agrees with the trend observed above, whereas the fact that GSH is not able to trigger gel formation indicates that the disulfide cleavage becomes unfavorable under these conditions. We hypothesize that the redox potential of GSH half-reaction is off-range for the RSStBu half-reaction and/or that the steric hindrance of RSStBu rest is too big for the disulfide cleavage by GSH. This result suggests that the specific combination of the molecular structure of the protecting group and the reductant type determinee gelation onset and kinetics, with gelation

times spanning from seconds to minutes, or even to hours range. This redox-responsive system with on-demand crosslinking provides flexible working conditions for gel preparation.

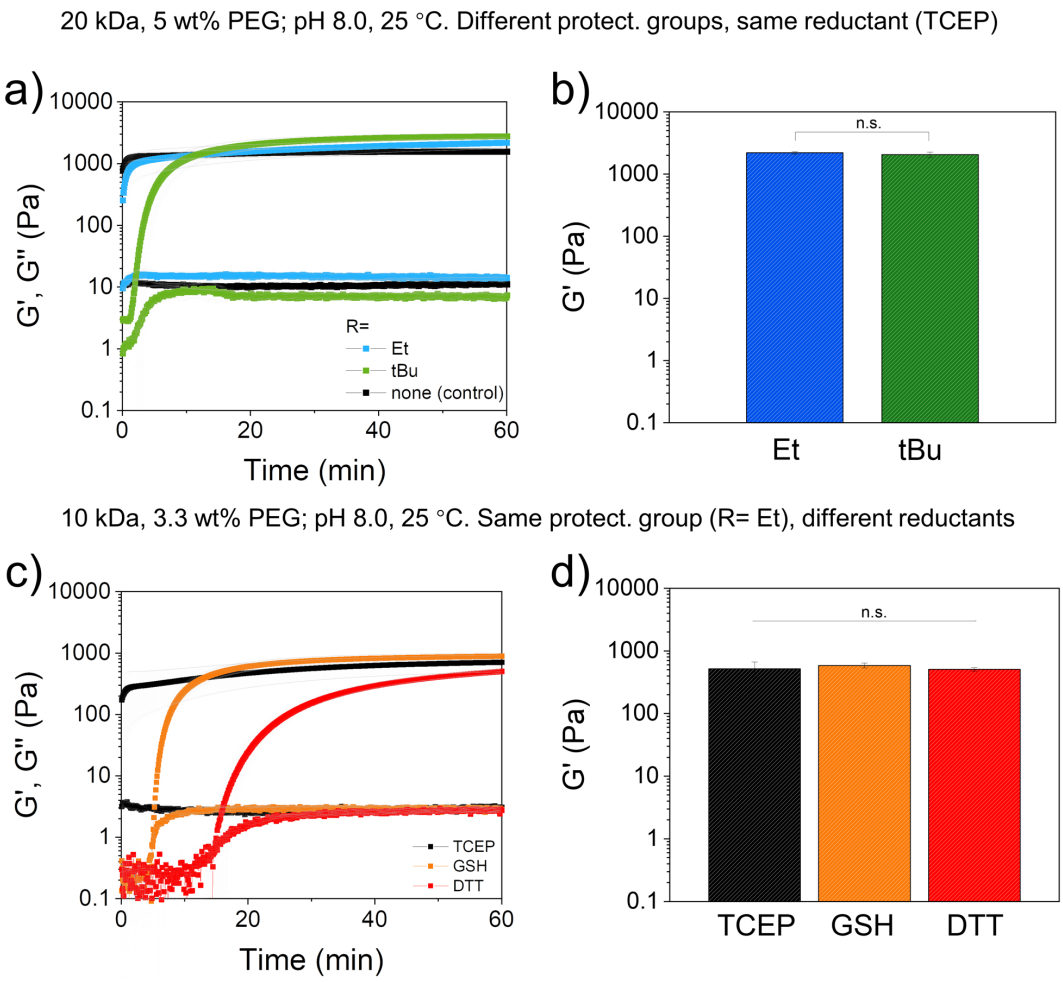

Figure 2. Study of gelation kinetics and mechanical strength of redox-triggered hydrogels by shear oscillatory rheometry, at varying Cys protecting group and reductant type. Shear storage (G′) and loss (G″) moduli were followed as a function of time. **a-b)** Effect of different Cys-protecting groups on PEG-Cys(SR) precursor, R= Et or tBu; on the gelation of CBT-Cys(SR) gels under constant reductant type (TCEP), before (a) and after (b) swelling. A CBT-Cys gel, prepared from unprotected PEG-Cys is shown as control. **c-d)** Effect of reductant type (TCEP, GSH or DTT) on the gelation kinetics and mechanical strength of CBT-Cys(SEt) gels, before

(c) and after (d) swelling (i.e., at constant protecting group). Gel composition: a-b) 20 kDa PEGs, 5 wt% polymer content, in HEPES buffer, at (1:1) reductant:Cys(SR) molar ratio, T= 25°C. c-d) 10 kDa PEGs, 3.3 wt% polymer content, in HEPES, at (1:1) reductant:Cys(SEt) molar ratio, T= 25°C. The reductant used is indicated in each case. In all cases, data are plotted as mean ± SD, n=3. In b) & d), statistical significance was analyzed by ANOVA followed by the post-hoc Tukey test (*$p < 0.05$ set for statistical significance level; n.s.= not significant).

Adjustment of environmental conditions within close-to-physiological range can be used to regulate materials properties

We investigated the possibility to adjust environmental cues, such as pH and temperature, within close-to-physiological range as a means of modulating gelation rate of CBT-Cys(SR) systems. To this end, CBT-Cys(SR) hydrogels were prepared at 5 wt% using TCEP as reductant, in buffer of varying pH (pH = 8 or 7) and at varying temperature (T= 25 or 37 °C); and rheological characterization was performed. Close-to-physiological range was chosen since our final goal is to implement the redox-triggered hydrogel platform for encapsulation of living cells within injectable matrices for different biomedical applications. Time-sweep experiments revealed a slower gelation rate when pH decreased from 8 to 7. CBT-Cys(SEt) gel formed in 30 s and 42 s (~1.4-fold slower), while CBT-Cys(StBu) gel formed in 1.7 and 7 min (~4.1-fold slower), when the pH decreased from 8 to 7, respectively (**Figure 3a**). This effect of pH on gelation kinetics could be attributed to two possibilities: i) the disulfide cleavage by TCEP is less efficient at lower pH, or ii) after disulfide cleavage and free thiol exposure of Cys group, the rate of luciferin ligation develops slower at lower pH, because of the smaller thiolate:thiol ratio. It is hypothesized that the second possibility dominates, in line with our previous work

on CBT-Cys gels,[27] and considering that TCEP has been reported to cleave disulfide bonds efficiently over a broad pH range from 9.0 to 1.5.[45]

To check whether different gelation rate regulated by pH additionally influences the final mechanical strength of the materials, gels at different pH values were prepared and G' after equilibrium swelling were compared. G' ranged 1710-2202 Pa and no significant difference was obtained across different pH values and protecting groups (Fig. S3). These results are in good agreement with a previous report on CBT-Cys system,[27] and prove the possibility of pH-regulating the gelation rate of redox-triggered CBT-Cys(SR) hydrogels, without affecting final gel mechanics.

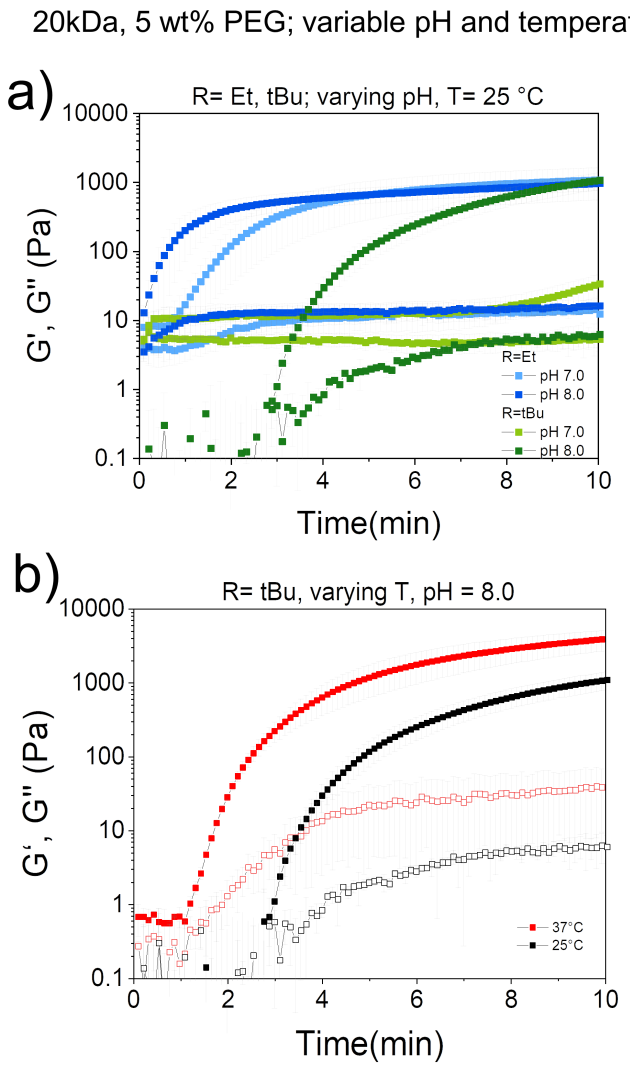

Figure 3. Study of gelation kinetics of TCEP-triggered CBT-Cys(SR) hydrogels by shear oscillatory rheometry at varying pH and temperature. **a)** Effect of pH on gelation kinetics of CBT-Cys(SR) gels. **b)** Effect of temperature on the gelation of CBT-Cys(StBu) system. Gel composition: 20 kDa PEGs, 5 wt% polymer content, in HEPES, at (1:1) TCEP:Cys(SR) molar ratio. Specific pH and temperature are indicated in each case. In all cases, data are plotted as mean ± SD, n=3.

Moreover, the effect of temperature on gelation rate was studied in CBT-Cys(StBu) system, the slowest of the series. In this case, gelation time decreased from 7 min to 1 min (7-fold faster) when the curing temperature increased from 25 to 37 °C (Fig. 3b). Importantly, temperature adjustment also impacted gel's mechanical strength: G'= 1072 Pa vs G'= 3879 Pa when curing was performed at 25 and 37 °C, respectively. This evidences that the increase of temperature also impacted the crosslinking degree of the formed networks, in good agreement with previous reports of other hydrogels which crosslinking was based on nucleophilic thiol-mediated coupling reactions.[46, 47]

Besides varying the molecular structure of the protecting group at Cys precursor, the reductant type, and the environmental conditions, adjustment of polymer content in the gel formulation can also be used to regulate materials properties. For instance, as demonstrated on Table S1 (see ESI), gelation rate of CBT-Cys(SR) gels can be tuned between seconds, minutes, and hours, depending on the specific choice of molecular and environmental parameters of the CBT-Cys(SR) system. Overall, the flexible redox-triggering of these materials upgrades the tunability of luciferin-inspired hydrogels.

Redox-triggered hydrogels are cytocompatible

To assess the feasibility of applying the redox-triggered CBT-Cys(SR) gels for cell-encapsulation, the cytocompatibility of these systems was studied. A procedure schematically shown in **Figure 4a** was followed. First, PEG-CBT precursor was biofunctionalized with the cell-adhesive cyclo(RGDfK(C)) peptide and then pre-mixed with the PEG-Cys(SR) precursor and human mesenchymal stem cells (hMSC) suspension. To this mixture, TCEP reductant solution was added to trigger the crosslinking process that led to the obtention of hydrogels with embedded cells. The final gel composition was 3 wt% PEG and 0.03 wt% (0.46 mM) cyclo(RGDfK(C)) peptide. Although at this composition gelation time was 30 s and 1 min for CBT-Cys(SEt) vs CBT-Cys(StBu) gels, respectively, hydrogels were left curing for 15 min in incubator. Moreover, note that luciferin ligation is used both for biofunctionalization of PEG chains and for gelation.

Embedded cells were cultured for 1 day, live/dead assay was performed, and cell viability was quantified (Fig. 4 b-e). Cells encapsulated in CBT-Cys(SR) hydrogels maintained high viability (>83%), similar to the value observed in CBT-Cys control gels and in good agreement with other established hydrogel systems for cell encapsulation, such as the thiol-vinylsulfone materials demonstrated in previous reports.[27, 46] These results prove that the use of TCEP as redox-trigger of gelation does not negatively impact cell survival, at least within the tested conditions (here, TCEP concentration was 2.8 mM). This demonstrates the good cytocompatibility of CBT-Cys(SR) hydrogels.

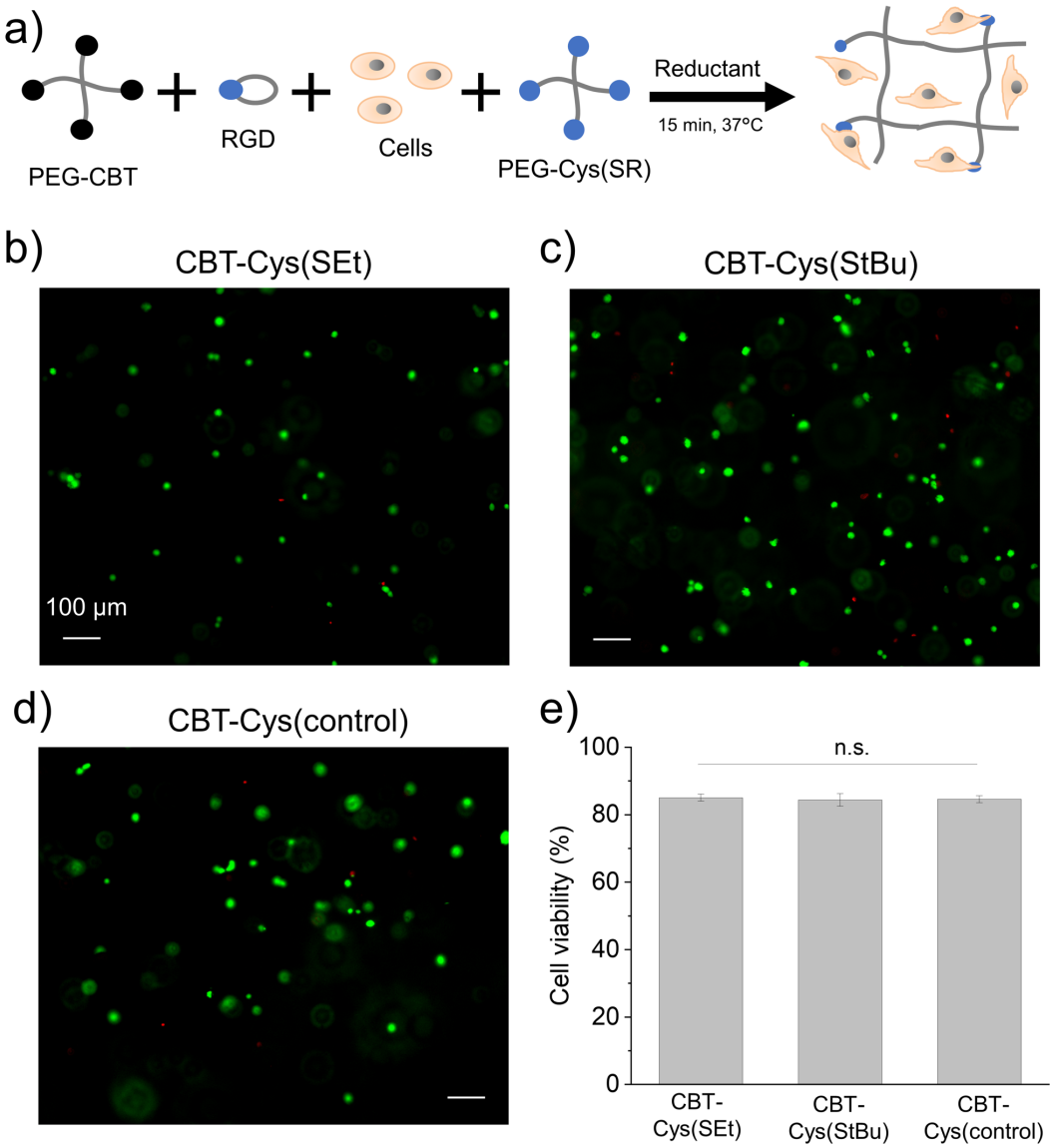

Figure 4. Cytocompatibility study of CBT-Cys(SR) hydrogels biofunctionalized with cell-adhesive cyclo(RGDfK(C)) peptide. a) Scheme of procedure followed for cell encapsulation, including biofunctionalization of PEG-CBT with RGD followed by redox-triggered crosslinking and cell encapsulation. **b-d)** Representative images showing post-encapsulation hMSCs survival after live (green)/dead (red) staining at 1 day of culture, and **e)** corresponding quantification of cell viability, at varying protecting groups CBT-Cys(SR) b) R= Et, c) R= tBu. d) A CBT-Cys control gel is shown for comparison. Scale bars: 100 µm. Statistical analysis was performed by ANOVA followed by post-hoc Tukey test (*$p < 0.05$ used for statistical

significance; n.s. = not significant). Gel composition: 20 kDa, 3 wt% PEGs, 0.03 wt% (0.5 mM) cyclo(RGDfK(C)), starting cell density per gel was 5000 cells.

Redox-triggering can be used for formulating injectable and in-bath crosslinkable hydrogel matrices

Injectable matrices for therapeutic delivery and tissue repair, either alone or in combination with processing and scaffolding technologies (e.g., extrusion-based printing), are becoming increasingly important for tissue engineering and regenerative medicine.[48, 49] These scenarios entail the delivery of low viscous (pre)mixed precursor solutions through a fine needle or nozzle to the application site, followed by on-demand quick gelation step for mechanical stabilization that is typically triggered by the action of an external stimulus[50, 51] We foresaw that the redox-triggerable luciferin-inspired hydrogel platform could be easily adapted towards injectable and in-bath crosslinking scenarios, thus combining the advantage of tunability of materials properties with the ease of processing such matrices.

To prove this concept, an experiment to test injectability and in situ in-bath crosslinking of our materials was designed (**Figure 5a**). 10 wt% PEG-CBT and PEG-Cys(SEt) precursors were pre-mixed and colored with green food dye for visualization purposes. The precursors mixture was injected via micropipette into a reductant bath that contained TCEP and buffer/glycerol equivolume combination. Note that glycerol was added to adjust the viscosity of the bath to better support the aimed crosslinked material. The precursors mixture could be injected through the fine pipette tip without clogging into the bath, and formation of a hydrogel was observed within 10 s (Fig. 5b and VideoS1 in ESI). After in-bath crosslinking and removal of the reductant bath, a hydrogel with good mechanical stability was obtained (Fig. 5c). A control

experiment was performed, in which PEG precursors were injected into a bath that contained buffer/glycerol but lacked the reductant. In this case, the precursors mixture rapidly dissolved in the bath and no hydrogel was formed (Fig. 5d and VideoS2 in ESI), demonstrating that solely the presence of reductant can trigger in-bath gelation.

As demonstrated in a previous section of this article, the good stability of aqueous solutions of PEG-Cys(SR) precursors facilitates the preparation of stock solutions, which can be pre-mixed with PEG-CBT precursor at a convenient time before processing the mixture for on-demand crosslinking. We anticipate that the redox-triggered hydrogel platform will be advantageous for the development of injectable matrices for drug delivery as well as bioinks for extrusion-based 3D printing.

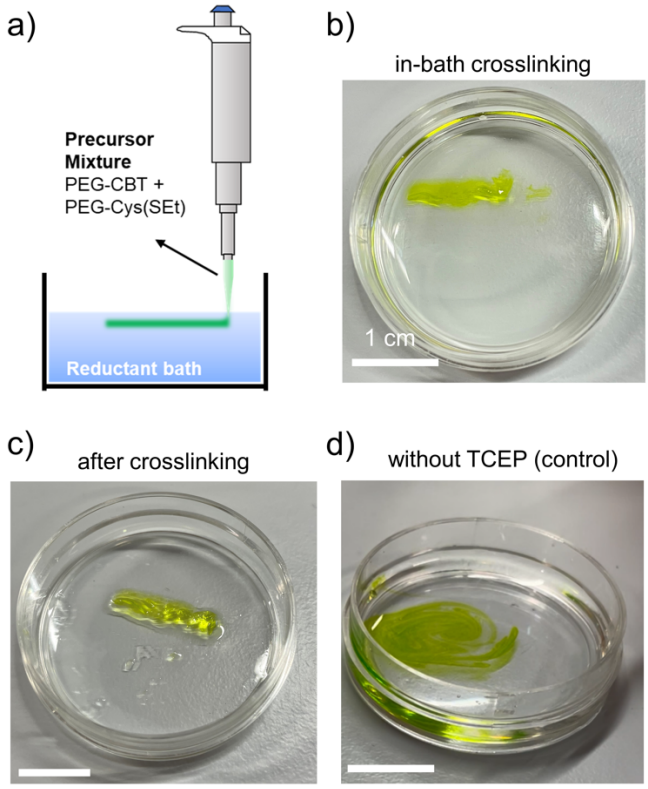

Figure 5. Demonstration of the use of redox-triggered gelation for developing injectable and in-bath crosslinkable hydrogel matrices. A solution mixture containing PEG-CBT and PEG-Cys(SEt) precursors was injected into a reductant bath, and CBT-Cys(SEt) gelation was triggered in situ. **a)** Schematics of experimental setup. **b)** Crosslinking of CBT-Cys(SEt) hydrogel in the reductant bath (TCEP was used). **c)** Hydrogel after in-bath crosslinking followed by removal of the reductant bath. **d)** Negative control: injecting precursors mixture in a bath without TCEP did not lead to the formation of a hydrogel. Instead, PEGs solution gets diluted in the bath. Precursors solutions: 10 kDa, 10 wt% PEG-CBT and 10 wt% PEG-Cys(SEt), (1:1) volume ratio in HEPES pH 8.0 (containing green food dye for clear visualization). Reductant bath: HEPES: glycerol (1:1) volume ratio, 20 mM TCEP. Scale bar: 10 mm. b-d) Snapshots of videos recorded during the experiments. The full videos can be found as ESI.

3. Conclusions

A novel redox-triggered luciferin-inspired hydrogel platform was developed in this work. PEG-Cys(SR) precursors demonstrated good storage stability in aqueous solution, which is expected to facilitate applicability of this platform in those settings requiring pre-mixing of reactive precursors. The CBT-Cys(SR) system allows flexible in situ gelation, whereby gelation onset and rate can be fine modulated by adjustment of intrinsic parameters (e.g., protecting group structure, reductant) and environmental parameters (e.g., pH and temperature) of the deprotection reaction. Depending on the specific choice of conditions, gelation times spanning from seconds to minutes to hours could be easily achieved. Furthermore, stem cells encapsulated in biofunctionalized CBT-Cys(SR) hydrogels showed high viability after 1 day of encapsulation, demonstrating the good cytocompatibility of these systems. With redox-triggered gelation, this smart hydrogel platform is envisioned as injectable matrices for drug

delivery and tissue engineering as well as inks for extrusion-based printing of soft constructs for regenerative medicine. These bioinspired materials with upgraded tunability expand the toolkit of stimuli-responsive materials.

Electronic Supplementary Information (ESI)

Supplementary results including ^{1}H NMR and rheological characterization, and experimental section.

Authors contributions

M.J. and A.G. synthesized macromer precursors and performed rheological characterization experiments. M.J. performed microscopy and cell experiments. M.J. and J.I.P wrote the initial manuscript. J.I.P. conceived and supervised the project, and acquired funding. All authors contributed with data analysis. All authors provided critical feedback on the manuscript and approved its final version.

Conflicts of interest

There are no conflicts of financial intertest to declare.

Acknowledgements

The authors thank financial support from the Deutsche Forschungsgemeinschaft (DFG, project no. 422041745) awarded to J.I.P. The authors thank Gülistan Koçer (INM) for supporting cell experiments and Prof. A. del Campo (INM) for mentoring and support.

References

1. K. Y. Lee and D. J. Mooney, *Chemical Reviews*, 2001, **101**, 1869-1880.
2. D. Seliktar, *Science*, 2012, **336**, 1124-1128.
3. I. Willner, *Accounts of Chemical Research*, 2017, **50**, 657-658.
4. F. Gao, Y. Zhang, Y. Li, B. Xu, Z. Cao and W. Liu, *ACS Applied Materials & Interfaces*, 2016, **8**, 8956-8966.
5. J. A. Burdick, D. Frankel, W. S. Dernell and K. S. Anseth, *Biomaterials*, 2003, **24**, 1613-1620.
6. M. Villiou, J. I. Paez and A. del Campo, *ACS Applied Materials & Interfaces*, 2020, **12**, 37862-37872.
7. A. Farrukh, J. I. Paez and A. del Campo, *Advanced Functional Materials*, 2019, **29**, 1807734.
8. L. Klouda, *European Journal of Pharmaceutics and Biopharmaceutics*, 2015, **97**, 338-349.
9. L. Klouda and A. G. Mikos, *European Journal of Pharmaceutics and Biopharmaceutics*, 2008, **68**, 34-45.
10. I. Tomatsu, K. Peng and A. Kros, *Advanced Drug Delivery Reviews*, 2011, **63**, 1257-1266.
11. Z. Liu, J. Liu, X. Cui, X. Wang, L. Zhang and P. Tang, *Frontiers in Chemistry*, 2020, **8**.
12. M. Antman-Passig and O. Shefi, *Nano Letters*, 2016, **16**, 2567-2573.
13. S. Kennedy, J. Hu, C. Kearney, H. Skaat, L. Gu, M. Gentili, H. Vandenburgh and D. Mooney, *Biomaterials*, 2016, **75**, 91-101.
14. D. Schmaljohann, *Advanced Drug Delivery Reviews*, 2006, **58**, 1655-1670.
15. N. A. Peppas and D. S. Van Blarcom, *Journal of Controlled Release*, 2016, **240**, 142-150.
16. R. Y. Tam, L. J. Smith and M. S. Shoichet, *Accounts of Chemical Research*, 2017, **50**, 703-713.
17. M. D. Konieczynska and M. W. Grinstaff, *Accounts of Chemical Research*, 2017, **50**, 151-160.
18. V. Yesilyurt, M. J. Webber, E. A. Appel, C. Godwin, R. Langer and D. G. Anderson, *Advanced Materials*, 2016, **28**, 86-91.
19. H. L. Lim, Y. Hwang, M. Kar and S. Varghese, *Biomaterials Science*, 2014, **2**, 603-618.
20. N. Eslahi, M. Abdorahim and A. Simchi, *Biomacromolecules*, 2016, **17**, 3441-3463.
21. X. Sui, X. Feng, M. A. Hempenius and G. J. Vancso, *Journal of Materials Chemistry B*, 2013, **1**, 1658-1672.
22. B. D. Fairbanks, S. P. Singh, C. N. Bowman and K. S. Anseth, *Macromolecules*, 2011, **44**, 2444-2450.
23. M. E. Bracchi, G. Dura and D. A. Fulton, *Polymer Chemistry*, 2019, **10**, 1258-1267.
24. Z. Gao, B. Golland, G. Tronci and P. D. Thornton, *Journal of Materials Chemistry B*, 2019, **7**, 7494-7501.
25. L. Wu, S. Di Cio, H. S. Azevedo and J. E. Gautrot, *Biomacromolecules*, 2020, **21**, 4663-4672.
26. M. Huo, J. Yuan, L. Tao and Y. Wei, *Polymer Chemistry*, 2014, **5**, 1519-1528.
27. M. Jin, G. Koçer and J. I. Paez, *ACS Applied Materials & Interfaces*, 2022, **14**, 5017-5032.
28. A. K. Mahanta and P. Maiti, *ACS Appl Bio Mater*, 2019, **2**, 5415-5426.

29. J. I. Paez, O. Ustahüseyin, C. Serrano, X.-A. Ton, Z. Shafiq, G. K. Auernhammer, M. d'Ischia and A. del Campo, *Biomacromolecules*, 2015, **16**, 3811-3818.
30. D. Bermejo-Velasco, A. Azémar, O. P. Oommen, J. Hilborn and O. P. Varghese, *Biomacromolecules*, 2019, **20**, 1412-1420.
31. J. Feng, X.-A. Ton, S. Zhao, J. I. Paez and A. Del Campo, *Biomimetics*, 2017, **2**, 23.
32. G. Liang, H. Ren and J. Rao, *Nature Chemistry*, 2010, **2**, 54-60.
33. P. K. Pullela, T. Chiku, M. J. Carvan and D. S. Sem, *Analytical Biochemistry*, 2006, **352**, 265-273.
34. M. Kar, Y.-R. Vernon Shih, D. O. Velez, P. Cabrales and S. Varghese, *Biomaterials*, 2016, **77**, 186-197.
35. S. E. Boiadjiev and D. A. Lightner, *Journal of the American Chemical Society*, 2000, **122**, 11328-11339.
36. T. J. Bechtel and E. Weerapana, *PROTEOMICS*, 2017, **17**, 1600391.
37. E. B. Getz, M. Xiao, T. Chakrabarty, R. Cooke and P. R. Selvin, *Analytical Biochemistry*, 1999, **273**, 73-80.
38. V. Ribas, C. García-Ruiz and J. C. Fernández-Checa, *Frontiers in Pharmacology*, 2014, **5**.
39. W. W. Cleland, *Biochemistry*, 1964, **3**, 480-482.
40. E. A. Dergousova, I. Y. Petrushanko, E. A. Klimanova, V. A. Mitkevich, R. H. Ziganshin, O. D. Lopina and A. A. Makarov, *Biomolecules*, 2017, **7**, 18.
41. K. Khazim, D. Giustarini, R. Rossi, D. Verkaik, J. E. Cornell, S. E. D. Cunningham, M. Mohammad, K. Trochta, C. Lorenzo, F. Folli, S. Bansal and P. Fanti, *Translational Research*, 2013, **162**, 16-25.
42. J. A. Burns, J. C. Butler, J. R. Moran and G. M. Whitesides, *Journal of Organic Chemistry*, 1991, **56**, 2648-2650.
43. Z. Zheng, P. Chen, G. Li, Y. Zhu, Z. Shi, Y. Luo, C. Zhao, Z. Fu, X. Cui, C. Ji, F. Wang, G. Huang and G. Liang, *Chemical Science*, 2017, **8**, 214-222.
44. V. Domkin and A. Chabes, *Scientific Reports*, 2014, **4**, 5539.
45. J. C. Han and G. Y. Han, *Analytical Biochemistry*, 1994, **220**, 5-10.
46. J. I. Paez, A. Farrukh, R. Valbuena-Mendoza, M. K. Wlodarczyk-Biegun and A. Del Campo, *ACS Appl Mater Interfaces*, 2020, **12**, 8062-8072.
47. N. J. Darling, Y.-S. Hung, S. Sharma and T. Segura, *Biomaterials*, 2016, **101**, 199-206.
48. J. H. Lee, *Biomaterials Research*, 2018, **22**, 27.
49. E. Lepowsky, M. Muradoglu and S. Tasoglu, *Bioprinting*, 2018, **11**, e00034.
50. I. T. Ozbolat and M. Hospodiuk, *Biomaterials*, 2016, **76**, 321-343.
51. L. Yu and J. Ding, *Chemical Society Reviews*, 2008, **37**, 1473-1481.